Constraining a physically based Soil-Vegetation-Atmosphere Transfer model with surface water content and thermal infrared brightness temperature measurements using a multiobjective approach

J Demarty, Catherine Ottle, Isabelle Braud, Albert Olioso, J. P. Frangi, H. V. Gupta, L. A. Bastidas

▶ **To cite this version:**

J Demarty, Catherine Ottle, Isabelle Braud, Albert Olioso, J. P. Frangi, et al.. Constraining a physically based Soil-Vegetation-Atmosphere Transfer model with surface water content and thermal infrared brightness temperature measurements using a multiobjective approach. Water Resources Research, 2005, 41 (1), pp.1-15. 10.1029/2004WR003695 . hal-01863535

HAL Id: hal-01863535
https://hal.science/hal-01863535

Submitted on 12 Sep 2020

HAL is a multi-disciplinary open access archive for the deposit and dissemination of scientific research documents, whether they are published or not. The documents may come from teaching and research institutions in France or abroad, or from public or private research centers.

L'archive ouverte pluridisciplinaire **HAL**, est destinée au dépôt et à la diffusion de documents scientifiques de niveau recherche, publiés ou non, émanant des établissements d'enseignement et de recherche français ou étrangers, des laboratoires publics ou privés.

Constraining a physically based Soil-Vegetation-Atmosphere Transfer model with surface water content and thermal infrared brightness temperature measurements using a multiobjective approach

Jérôme Demarty,[1,2] Catherine Ottlé,[1] Isabelle Braud,[3,4] Albert Olioso,[2] Jean Pierre Frangi,[5] Hoshin V. Gupta,[6] and Luis A. Bastidas[7]

Received 30 September 2004; accepted 4 November 2004; published 20 January 2005.

[1] This article reports on a multiobjective approach which is carried out on the physically based Soil-Vegetation-Atmosphere Transfer (SVAT) model. This approach is designed for (1) analyzing the model sensitivity to its input parameters under various environmental conditions and (2) assessing input parameters through the combined assimilation of the surface water content and the thermal infrared brightness temperature. To reach these goals, a multiobjective calibration iterative procedure (MCIP) is applied on the Simple Soil Plant Atmosphere Transfer–Remote Sensing (SiSPAT-RS) model. This new multiobjective approach consists of performing successive contractions of the feasible parameter space with the multiobjective generalized sensitivity analysis algorithm. Results show that the MCIP is an original and pertinent approach both for improving model calibration (i.e., reducing the a posteriori preferential ranges) and for driving a detailed SVAT model using various calibration data. The usefulness of the water content of the upper 5 cm and the thermal infrared brightness temperature for retrieving quantitative information about the main input surface parameters is also underlined. This study opens perspectives in the combined assimilation of various multispectral remotely sensed observations, such as passive microwaves and thermal infrared signals.

Citation: Demarty, J., C. Ottlé, I. Braud, A. Olioso, J. P. Frangi, H. V. Gupta, and L. A. Bastidas (2005), Constraining a physically based Soil-Vegetation-Atmosphere Transfer model with surface water content and thermal infrared brightness temperature measurements using a multiobjective approach, *Water Resour. Res.*, *41*, W01011, doi:10.1029/2004WR003695.

1. Introduction

[2] Monitoring energy and water exchanges between the soil, the vegetation and the atmosphere is important for meteorological, agronomical and hydrological purposes. Models designed for simulating these exchanges are the so-called Soil-Vegetation-Atmosphere Transfer (SVAT) models. They require a large set of input parameters and initial conditions describing surface properties that must be correctly specified for providing accurate assessment of the energy and water fluxes. Most of these properties vary in time and space and are often assessed through in situ experiments. For example, SVAT models based on Darcian flow require information about the soil hydraulic characteristics that define the relationships between hydraulic conductivity, soil matric potential, and soil water content. The experimental techniques to assess soil hydraulic properties are time consuming, expensive and generally limited by the large spatial variability of these properties. Pedo-transfer functions, relating the soil hydraulic properties to soil data available from soil surveys, were alternatively developed to estimate empirically soil water retention and conductivity. However, these functions were developed from a very limited number of soils and the correlations are often weak and location specific [*Burke et al.*, 1997]. Same difficulties occurred for most of the other surface properties (vegetation surface conductance, thermal properties of soil, aerodynamic roughness), all of them being difficult to assess in situ. Alternative approaches based on remote sensing techniques may be able to provide indirect large-scale information about surface properties. In particular, it is now well established that L-band (1.4 GHz) passive microwave remotely sensed measurements are highly related to the surface soil moisture [*Jackson and Schmugge*, 1991; *Jackson et al.*, 1995, 1999] and canopy water amount [*Wigneron et al.*, 1996, 2002]. The potential of passive microwave data to assess quantitative

[1]Centre d'étude des Environnements Terrestre et Planétaires/Centre National de la Recherche Scientifique/Université de Versailles Saint-Quentin-en-Yvelines, Vélizy, France.
[2]Unité Climat, Sol et Environnement, Institut National de la Recherche Agronomique Avignon, Avignon, France.
[3]Laboratoire d'étude des Transferts en Hydrologie et Environnement/Centre National de la Recherche Scientifique/Institut National Polytechnique de Grenoble/Institut de Recherche pour le Développment/Université Joseph Fourier, UMR5564, Grenoble, France.
[4]Unité de Recherche Hydrologie-Hydraulique, Cemagref, Lyon, France.
[5]Laboratoire Environnement et Développement/Université Paris 7, Paris, France.
[6]Sustainability of Semi-arid Hydrology and Riparian Areas, Department of Hydrology and Water Resources, University of Arizona, Tucson, Arizona, USA.
[7]Department of Civil and Environmental Engineering, Utah State University, Logan, Utah, USA.

Copyright 2005 by the American Geophysical Union.
0043-1397/05/2004WR003695

information about surface properties used in a SVAT models was investigated in recent studies [*Burke et al.*, 1997, 1998; *Margulis et al.*, 2002; *Wigneron et al.*, 2002]. For instance, *Burke et al.* [1997, 1998] retrieved information about soil hydraulic properties used in a soil water and energy budget model, coupled with a microwave emission model from L-band brightness temperature measurements. More recently, *Wigneron et al.* [2002] assimilated L-band brightness temperature in the ISBA-Ags model [*Calvet et al.*, 1998], coupled with the Tau-Omega microwave radiative transfer model [*Wigneron et al.*, 1995], in order to retrieve initial soil moisture and a parameter controlling vegetation growth. Thermal infrared may also provide significant information about parameters controlling canopy processes, such as evapotranspiration. Since SVAT models are based on the resolution of the energy balance equation, the use of TIR was investigated in detail by many authors [*Soer*, 1980; *Carlson et al.*, 1990; *Camillo*, 1991; *Ottlé and Vidal-Madjar*, 1994; *Taconet et al.*, 1995; *Olioso et al.*, 1999a; *Margulis and Entekhabi*, 2003]. Although all the above cited studies demonstrated the potential of remotely sensed data for retrieving surface properties used in SVAT model, only few of them analyzed the synergy between various spectral domains [*Camillo*, 1991; *Ottlé and Vidal-Madjar*, 1994; *Clevers and van Leeuwen*, 1996; *Olioso et al.*, 1999b, 2001; *Cayrol et al.*, 2000; *Droogers and Bastiaanssen*, 2002].

[3] Generally, calibration in land surface modeling is considered as the determination of a single optimum parameter set, allowing the "best" simulation of several output variables. Owing to errors in model structure and parameter uncertainties, the determination of this set remains difficult, if not impossible. As a consequence, multiobjective approaches were developed in hydrology in order to isolate parameter sets that cannot be distinguished in terms of model performance [*Yapo et al.*, 1996, 1998; *Gupta et al.*, 1998]. The multiobjective approaches have already been applied in different modeling contexts, such as the multiobjective calibration of rainfall-runoff models [*Madsen*, 2000; *Boyle et al.*, 2000, 2001; *Vrugt et al.*, 2003a, 2003b], land surface models [*Gupta et al.*, 1999; *Houser et al.*, 2001; *Xia et al.*, 2002; *Leplastrier et al.*, 2002; *Vrugt et al.*, 2003a, 2003b] and an hydrochemical model [*Meixner et al.*, 2002]. A popular approach is the multiobjective complex evolution (MOCOM-UA) global optimization method, which solves the multiobjective calibration problem by combining the strengths of the complex shuffling strategy and downhill Simplex evolution with the concept of Pareto dominance [*Yapo et al.*, 1998]. It aims to isolate parameter sets having the property that moving from one solution to another results in the improvement of one objective while causing deterioration in one or more others one (also called the Pareto set, see section 2). Results obtained in the above mentioned studies showed that MOCOM-UA can provide an estimate of the Pareto set. However, *Gupta et al.* [2003] discussed recently on the tendency of the MOCOM-UA algorithm both to cluster the solutions into a central compromise region of the Pareto set and to converge prematurely for case studies involving larger numbers of parameters and strongly correlated performance criteria. A similar behavior was found when the MOCOM-UA algorithm was tested on a simplified crop growth model by *Demarty et al.* [2004a], also showing that the part of the Pareto set in which the algorithm was converging was highly sensitive to the presence or not of some particular solutions. This problem even occurred in the case of a simple mathematical test done by *Vrugt et al.* [2003a]. Another limitation of the MOCOM-UA algorithm is induced by the very high number of model runs required by its implementation, typically greater than 100 000 [*Gupta et al.*, 1999], even in good situations such as using a previous sensitivity analysis allowing the reduction of the dimension of the optimization procedure [*Bastidas et al.*, 1999]. In the case of complex and non linear models, requiring the prescription of many surface properties and consuming significant computer time the efficiency of the MOCOM-UA algorithm could be highly impacted. In a recent study, *Demarty et al.* [2004b] proposed an alternative multiobjective approach for retrieving quantitative information used in a detailed SVAT model using the multiobjective generalized sensitivity analysis (MOGSA [*Bastidas et al.*, 1999]). MOGSA was originally developed to determine the main influential input parameters through a sensitivity analysis based on the concept of Pareto dominance. *Demarty et al.* [2004b] showed that MOGSA was also useful for retrieving quantitative information about these parameters and for assessing their a posteriori distributions (calibration). Nevertheless, these authors also showed that MOGSA could provide relatively large a posteriori parameter distributions in which the choice of a particular calibrated value was finally subjective. Moreover, the calibration was carried out on the a priori knowledge of five surface variables: soil heat flux {G}, sensible heat flux {H}, latent heat flux {LE}, water content of the upper 5 cm of soil $\{W_{05}\}$ and local thermal infrared brightness temperature $\{T_b\}$. Accounting for G, H and LE fluxes in the objective functions of the calibration procedure provided substantial information for constraining the SVAT model. This information is not available in a context where only remotely sensed observations were used to constrain the SVAT model. More generally and in spite of its ability to investigate synergy between various types of data, only few multiobjective approaches were applied in such a context of using remotely sensed data [*Crow and Wood*, 2003].

[4] In this study, we investigated the potential of remote sensing observations for assessing surface properties used in a detailed SVAT model. The study was carried out on the physically based Simple Soil Plant Atmosphere Transfer–Remote Sensing (SiSPAT-RS [*Braud et al.*, 1995; *Braud*, 2000; *Demarty et al.*, 2002, 2004b] (see http://www.lthe.hmg.inpg.fr)) model through the knowledge of the soil water content of the upper 5 cm (related to L-band microwave brightness temperature) and of the thermal infrared brightness temperature. These two variables were simultaneously used to calibrate the model using a new multiobjective parameter estimation procedure, called the multiobjective calibration iterative procedure (MCIP) and built upon the multiobjective calibration procedure proposed by *Demarty et al.* [2004b]. MCIP was developed both for complex model consuming significant computer time and for improving prediction of the a posteriori parameters distributions using various types of calibration data. It was based on a Monte Carlo iterative procedure allowing successive narrowing of the a posteriori parameter

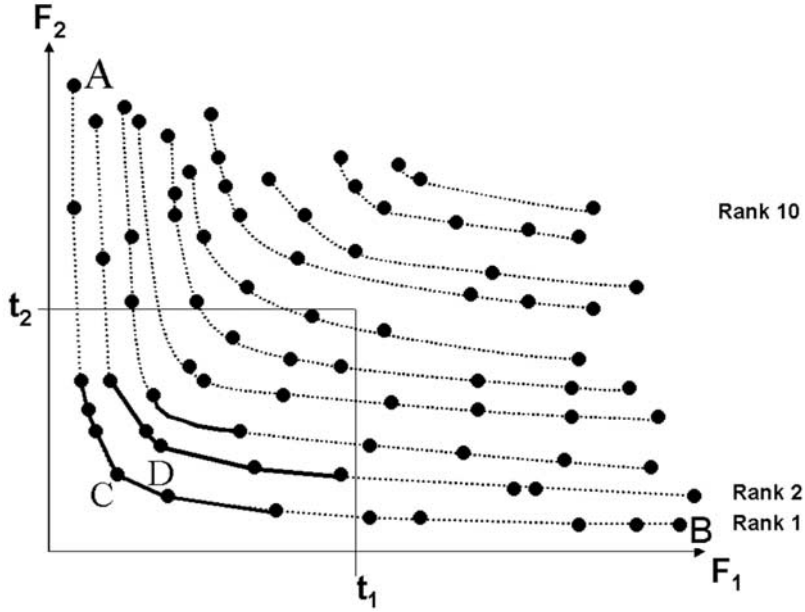

Figure 1. Pareto ranking with threshold in a case of two objectives functions $\{F_1, F_2\}$. Each point represents results of a particular simulation. A maximal rank of 10 was found. Partition into "acceptable" solutions (points linked by dark lines) and "nonacceptable" solutions (remaining points linked by dash lines) was realized considering a Pareto rank 3 and thresholds for each single objective function (t_1 and t_2).

ranges provided by the MOGSA algorithm. Compared to MOCOM-UA, this iterative procedure makes it possible to considerably reduce the number of model runs required for deriving the solution of the multiobjective calibration problem. The results were analyzed both in terms of input parameter retrieval and of impact on the simulated energy and water fluxes. The database acquired over a winter wheat field during the Alpilles-ReSeDA (Remote Sensing Data Assimilation [*Olioso et al.*, 2002a]) experiment was used in this study.

[5] The article is organized as follows. Section 2 describes the multiobjective approach which was performed on the SiSPAT-RS model. Section 3 provides an overview of the data set, the SiSPAT-RS model and the modeling strategy. Section 4 presents the results in terms of model sensitivity analysis, parameter retrievals and consequences on the simulated surface fluxes. Finally, the last section opens the article for discussion and conclusion.

2. Multiobjective Approach

2.1. Multiobjective Formulation and Pareto Set

[6] Generally speaking, the multiobjective problem can be stated as the following minimizing formulation [*Yapo et al.*, 1998]:

$$\mathrm{Min}\left\{F_1\left(\theta^j\right), F_2\left(\theta^j\right), \ldots, F_m\left(\theta^j\right)\right\}, \quad (1)$$

where F_i symbolizes a single objective function with i = 1, ..., m and $\theta^j = \{\theta_1^j, \theta_2^j, \ldots, \theta_p^j\}$ a particular set of p parameters included in the feasible parameter space. In practice, the solution of the multiobjective formulation given in equation (1) does not lead to a unique solution minimizing all criteria simultaneously [*Gupta et al.*, 1999]. Instead, a set of solution is commonly found, which is currently named Pareto set or "behavioral" set. Each solution in the Pareto set improves one or several criterion while causing deterioration of another, so it is not possible to isolate objectively the best solution among the "behavioral" solutions. Therefore within the Pareto set, none of the solutions is better than the other in terms of all objective functions. Examples of Pareto set were presented in several recent articles [e.g., *Gupta et al.*, 1999; *Houser et al.*, 2001; *Demarty et al.*, 2004a, 2004b].

2.2. MOGSA Algorithm

[7] The multiobjective generalized sensitivity analysis methodology (MOGSA [*Bastidas et al.*, 1999]) is a robust and efficient method for accounting for the joint multiparameter and multiresponse interactions. It is based on a Monte Carlo search of the feasible space (j = 1, ..., N in equation (1)) and on the notions of Pareto set and Pareto ranking [*Goldberg*, 1989]. The Pareto ranking determines first the Pareto set of the whole sample and assigns a rank 1 to its members. Setting aside these solutions, a new Pareto set is then determined for the remaining members of the sample, and a rank 2 is assigned to its members. The same procedure is applied until all the points of the sample have been processed. Lower ranks provide better results in a multiobjective sense. The choice of a rank as threshold allows the partition of the sample into the so-called "acceptable" and "nonacceptable" regions. On the other hand, *Leplastrier et al.* [2002] proposed to remove the extreme solutions of the "acceptable" regions which assured accurate results for only one criterion, by adding threshold values for each single objective function. Figure 1 shows an example of Pareto ranking, combined

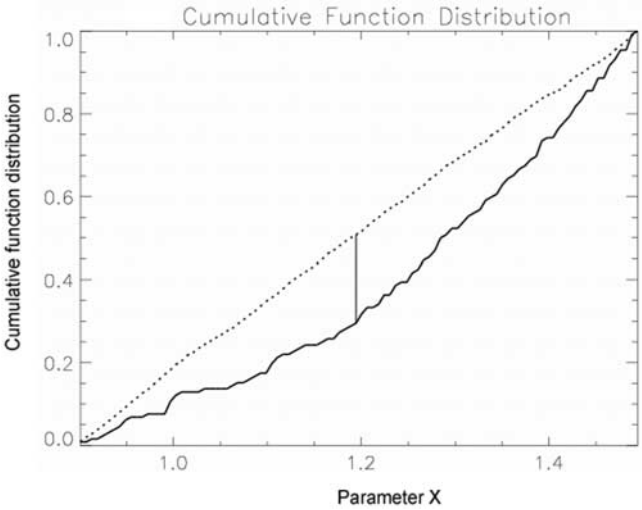

Figure 2. Comparison of cumulative marginal distribution functions of parameter *X* obtained for ''acceptable'' solutions (solid line) and ''nonacceptable'' solutions (dashed line). Vertical bar represents the maximum distance between the two cumulative distribution functions on which the Kolmogorov-Smirnov test is then applied.

to a threshold on each single objective function, in a simple case where only two objectives functions were considered. Points within the criterion space show model performance in terms of single objective functions $\{F_1, F_2\}$. The ranking procedure isolates 10 successive Pareto sets. The partition into the ''acceptable'' (points joins by the bold solid line) and the ''nonacceptable'' regions (remaining points) is finally done considering a Pareto rank 3 and two individuals thresholds (t_1 and t_2) for each single criteria.

[8] The statistical analysis of each parameter distributions between the ''acceptable'' and ''nonacceptable'' regions allows an assessment of model sensitivity to the parameter. In this context, the computation of the Kolmogorov-Smirnov (KS) two samples test is used to estimate whether the Cumulative Marginal Distribution Functions (CMDF) of the two regions are different. Significance levels for probability value can be chosen to define ''high,'' ''medium,'' and ''low'' parameter sensitivities [*Bastidas et al.*, 1999]. Figure 2a shows an example of CMDF obtained for a high sensitive parameter named *X*. The feasible space of *X* is [0.9; 1.5]. The dark and dotted lines indicate the CMDF obtained for acceptable solutions and nonacceptable solutions, respectively. The vertical dark line represents the maximum distance between the two distributions which is used in the KS two samples test.

2.3. Multiobjective Calibration Iterative Procedure (MCIP)

[9] In addition to the determination of the main influential parameters on the simulated variables, the MOGSA algorithm is potentially useful for retrieving quantitative information on these parameters [*Demarty et al.*, 2004a, 2004b]. This can be done through the analysis of the CMDF of the acceptable solutions. In particular, if the CMDF of the acceptable solutions increases uniformly, then the model is insensitive to this parameter (see section 2.2) and it is finally not possible to isolate preferential values in the a priori uncertainty range. Conversely, if the CMDF is concave (respectively convex), then it indicates more probability mass at higher (lower) values of the parameter. In such a case, it is possible to determine a new lower (upper) limit of the uncertainty range for the considered parameter. Such a limit coincides with the maximum distance between the two distributions which is used in the KS two samples test. Let us consider the previous example, Figure 2 shows that the CDFM is concave, and the 1.2 value of *X* appears to be statistically the lower limit for the acceptable solutions. As a consequence, *X* can be calibrated choosing a specific value in the a posteriori and preferential range [1.2; 1.5]. Such a simple approach was used by *Demarty et al.* [2004a, 2004b] for prescribing soil thermal and hydraulic properties. However, it can be relatively subjective, notably in the case of large preferential ranges. In order to avoid these types of problems, we proposed in the present study to apply an iterative procedure (Figure 3), based on the successive narrowing of the feasible parameter space. Each iteration was based on chaining the three following steps: (1) generation of a set of simulations from initial distributions of the input parameters, (2) analysis of the model sensitivity with the MOGSA algorithm and (3) determination of the preferential ranges of the most influential parameters, which were used to narrow the feasible space and to generate a new set of simulations in the next iteration. It is important to note that parameters, for which no model sensitivity is observed, are let free to vary in their initial uncertainty ranges for the next iteration. The implementation of this procedure, called multiobjective calibration iterative procedure (MCIP), is very simple. It allows the regular contraction of the feasible parameter space between iteration. The initial parameter distributions used in iteration 1 corresponded to the a priori parameter distributions. The procedure is ended when the new simulation set does not significantly contribute to the improvement of the minimized criteria. The final preferential uncertainty ranges allowed the assessment of the a posteriori parameter distributions. Furthermore, the use of threshold values for each single objective function in MOGSA (see section 2.2) can be useful to account for errors in observations and model in the calibration procedure.

[10] Although MCIP and the MOCOM-UA algorithm are based on similar bases and concept, the philosophy of the two multiobjective approaches is quite different. MCIP has not for vocation to determine the whole Pareto set. Instead, the iterative process makes the parameter space to evolve the parameter optimization in the direction of the feasible parameter space which provides the best model calibration, as in a classical optimization procedure (such as the Simplex). Nevertheless, MCIP still remains a real multiobjective approach, merging the strength of the Pareto dominance with computation efficiency. Moreover, it includes an internal sensitivity analysis which is very useful for a better investigation of the model structure, especially by analyzing the changes in model sensitivity with the successive contractions of the parameter feasible space. For all these reasons, MCIP seems particularly adapted to complex models, requiring the prescription of many input parameters and for which a calibration strategy requiring a

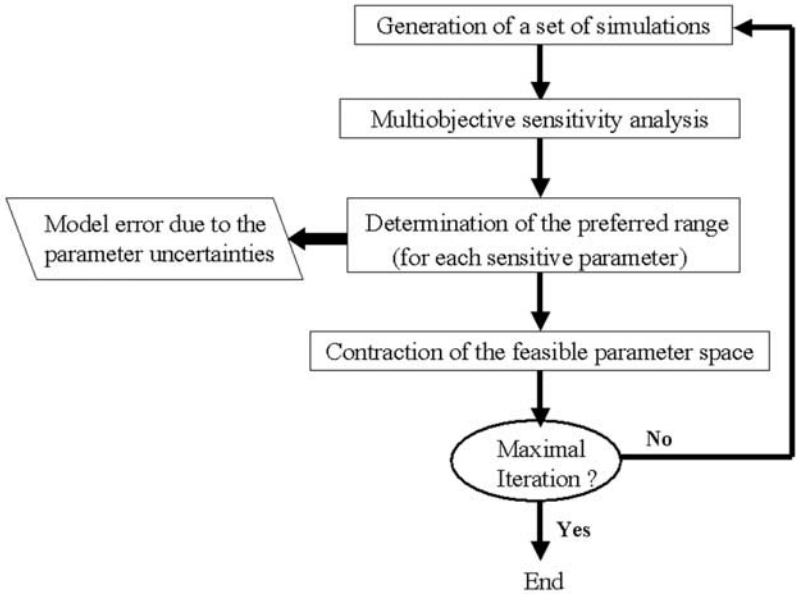

Figure 3. Schematic of the multiobjective calibration iterative procedure (MCIP) based on the multiobjective generalized sensitivity analysis (MOGSA) algorithm.

high number of simulations will be computationally less efficient.

3. Case Studies

[11] Using the MCIP, a multiobjective approach was performed on the SiSPAT-RS model. It was applied in a context of microwave and thermal infrared data assimilation through the combined assimilation of the two following variables: (1) the water content of the upper 5 cm of soil (W_{05}), which is highly correlated with the passive microwave brightness temperature at low frequencies (L-band), and (2) the thermal infrared brightness temperature (T_b). Objective functions associated to each of these variables were defined as the Root Mean Square Error (RMSE) between observed and simulated variables. In order to focus on canopy processes which occur during the day, observations acquired between 7 a.m. and 4 p.m., were accounted in the computation of the two objective functions.

[12] In this study, two main objectives were pursued through the multiobjective approach. First, we investigated how the model sensitivity varied along the year in relation with the climatic conditions and vegetative stage. Thus the MOGSA algorithm was first applied on two separate periods among the crop cycle. The first period (days of experiment (DOE) 440–460, 15 March to 4 April 1997) corresponded to a regular soil drying during the wheat-growing period. A very dry soil and a well-developed canopy characterized the second period (DOE 505–517; 19–31 May). According to the available measurements, it was unfortunately not possible to isolate more contrasted temporal windows in terms of environmental conditions (see section 3.3).

[13] Second, we investigated the best way to constrain the SVAT model using MCIP and the potential to retrieve quantitative information on the surface properties, notably on the soil hydraulic and thermal properties. MCIP was applied on the first period DOE 440–460 for which several Alpilles-ReSeDA observations were available for its validation.

3.1. Soil-Vegetation-Atmosphere Transfer (SVAT) Model

[14] The Simple Soil Plant Atmosphere Transfer model (SiSPAT [*Braud et al.*, 1995; *Braud*, 2000]), coupled with a Remote Sensing module (SiSPAT-RS [*Demarty et al.*, 2002, 2004a, 2004b]), was used in this study. This model describes vertical heat and water exchanges within the soil-plant-atmosphere continuum. It is a two-layer (soil and vegetation) SVAT model (Figure 4). The soil column is described as a juxtaposition of horizontal horizons, characterized by different thermal and hydraulic properties. Soil heat and mass transfers are coupled following the formalism proposed by *Milly* [1982]. The specification of retention curve and hydraulic conductivity parameterizations for each horizon in terms of volumetric water content is required. Water extraction from the soil by roots is parameterized using a resistance model developed by *Federer* [1979], considering that plant transpiration equals root extraction. The sensible and latent heat fluxes (H and LE) are expressed using an electrical analogy. The bulk stomatal resistance (r_s) is computed following *Jarvis* [1976] in terms of environmental factors (incoming solar radiation, vapor pressure deficit and leaf water potential). The three aerodynamic resistances (r_{as}, r_b, r_a) are calculated using the wind profile parameterizations inside and above the canopy proposed by *Shuttleworth and Gurney* [1990]. For a complete description of the SiSPAT model, see *Braud et al.* [1995] or *Braud* [2000].

[15] The SiSPAT-RS version was developed to improve the prediction of the modeled prognostic variables by assimilation of remote sensing data. For this purpose, the SVAT model was coupled with two Radiative Transfer

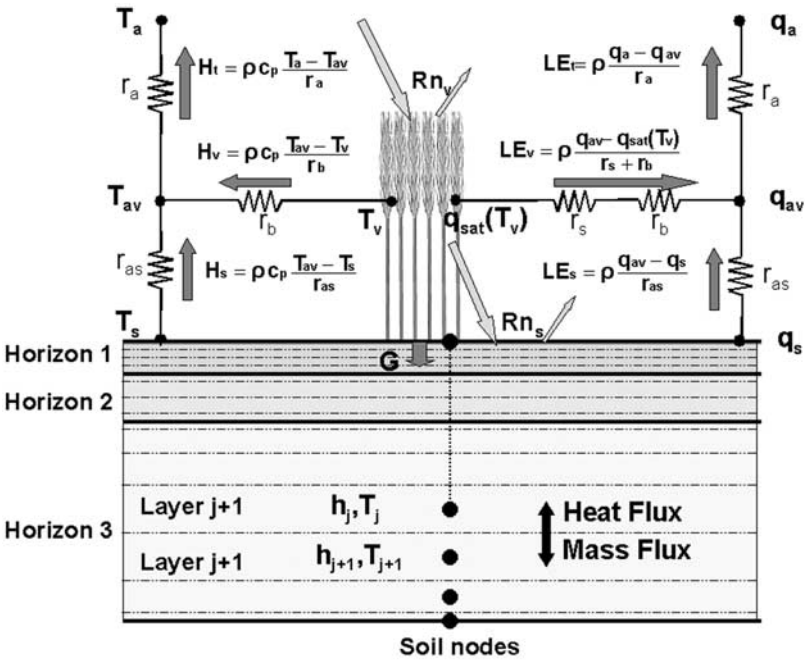

Figure 4. Schematic of the energy processes in the Simple Soil Plant Atmosphere Transfer (SiSPAT) model: net radiation (Rn), soil heat conduction (G), sensible and latent heat fluxes (H and LE), bulk stomatal resistance (r_s) and aerodynamic resistances (r_b, r_{as}, r_a), temperatures (T), and specific humidity (q). Subscripts, v, and t refer to the soil, vegetation, and total contributions, respectively; subscript a refers to the reference height measurements above the canopy, and subscript av refers to the fictive level inside the canopy.

Models (RTM) in the visible–near infrared and thermal infrared spectral domains. In the visible–near infrared spectral domain (0.3–3 μm), the 2M version (multilayer and multielement [*Weiss et al.*, 2001]) of the scattering by arbitrary inclined leaves (SAIL [*Verhoef*, 1984, 1985]) model was implemented in the SVAT model in order to simulate the bidirectional reflectances in the spectral and geometrical measurement conditions and the radiative exchanges between the soil, the vegetation and the atmosphere. The canopy was described as several horizontal layers of vegetation in specific phenological phases (green, yellow or senescent vegetation layer). Moreover, different vegetative organs, such as leaf, stem or ear, composed each layer of vegetation. Such a representation of the canopy required to account for the different vegetative layers into the SiSPAT structure. That was simply done by the specification of an organ area index to each vegetative organ, instead of using only the green Leaf Area Index (LAI) as in the original version. However, we assumed that each vegetative layer had a different contribution to the surface processes according to their associated phenological states. We considered that only green vegetation layers contributed to plant transpiration (through the bulk stomatal resistance) and that total vegetation, including green layers and yellow/senescent layers, contributed to radiative (through the shielding factor) and aerodynamic (through the aerodynamic resistances) processes.

[16] In the thermal infrared domain, a directional parameterization [*François et al.*, 1997] was coupled with the SiSPAT model. This parameterization simulated the spectral brightness temperature between 8–14 μm in a specific viewing configuration. It required the temperature of the soil surface and the temperature of the vegetation which were both simulated by the SiSPAT model.

3.2. Data Set

[17] The data set collected on a winter wheat field (numbered 101) of the Alpilles-ReSeDA experiment [*Olioso et al.*, 2002a] was used in this study. The aim of this experiment was to provide a consistent data set for assessing crop and soil processes using remote sensing data. It focused on agricultural land and practices. Therefore a small agricultural area, characterized by a large diversity of crops (wheat, sunflower, alfalfa), was instrumented and monitored during one year to document the whole crop cycle. The site was located near Avignon, France, (N43°47′, E4°45′) and the experiment lasted from October 1996 to November 1997. A very flat area, with fields of size 200 m by 200 m characterized the site. Atmospheric forcing was measured in the middle of the experimental area, over a bare soil surface with a 15 s time step and an averaging period of 20 min. The soil characterization of the field numbered 101, including particle size data, infiltration and dry bulk density measurements, were done at several depths along the soil profile. Canopy height, green Leaf Area Index (LAI) and Organ Area Index (OAI) for leaves, stems and ears in green vegetative phase and yellow/senescent vegetative phase were acquired regularly during the crop cycle and interpolated to daily values. Several initial and modeled output variables were observed, such as soil moisture down to a depth of 140 cm, energy and mass fluxes and local thermal infrared brightness temperatures (Table 1). Eddy correlation (EC) and Bowen ratio (BR) methods were implemented to assess latent and sensible heat fluxes over short periods and

Table 1. Uncertainty Ranges Associated With Each of the 35 Input Parameters of the Simple Soil Plant Atmosphere Transfer–Remote Sensing (SiSPAT-RS) Model[a]

	Parameter	Uncertainty Boundary Range			
		Initial	Intermediate (MOGSA)	Final (MCIP)	Observed
	Van Genuchten Retention Curve				
Wsa_1	saturated water content for H_1, $m^3\ m^{-3}$	0.37–0.53	0.37–0.45	0.40–0.43	*0.43*
Wsa_2	saturated water content for H_2, $m^3\ m^{-3}$	0.37–0.43	0.39–0.43	0.39–0.42	*0.41*
Wsa_3	saturated water content for H_3, $m^3\ m^{-3}$	0.37–0.40	. . .	0.37–0.39	*0.38*
hg_1	scale factor in the VG retention curve model for H_1, m	−2.0 to −0.02	−0.8 to −0.3	−0.6 to −0.3	*−0.4*
hg_2	scale factor in the VG retention curve model for H_2, m	−3.5 to −0.6	. . .	−1.8 to −1.2	*−0.8*
hg_3	scale factor in the VG retention curve model for H_3, m	−5.0 to −2.5	−3.5 to −2.5	−3.5 to −2.5	*−3.0*
n_1	shape parameter in the VG retention model for H_1	2.116–2.151	2.13–2.151	2.13–2.145	*2.129*
n_2	shape parameter in the VG retention model for H_2	2.115–2.145	. . .	2.125–2.145	*2.133*
n_3	shape parameter in the VG retention model for H_3	2.110–2.145	2.125–2.145	2.125–2.145	*2.136*
	Hydraulic and Thermal Soil Properties				
Ks_1	saturated liquid hydraulic conductivity for H_1, m s^{-1}	5×10^{-10}–5.10^{-6}	1×10^{-7}–5×10^{-6}	5×10^{-7}–2×10^{-6}	5.0×10^{-7}
Ks_2	saturated liquid hydraulic conductivity for H_2, m s^{-1}	2×10^{-10}–2×10^{-6}	. . .	1×10^{-7}–2×10^{-6}	2.0×10^{-7}
Ks_3	saturated liquid hydraulic conductivity for H_3, m s^{-1}	2×10^{-10}–2×10^{-6}	1×10^{-8}–5×10^{-7}	1×10^{-8}–6.5×10^{-8}	5.0×10^{-8}
La_1	multiplicative coef. of thermal conductivity for H_1	0.4–4.0	0.4–0.8	0.4–0.55	0.5
La_2	multiplicative coef. of thermal conductivity for H_2	0.5–4.0	0.5–1.5	0.5–0.8	1.0
La_3	multiplicative coef. of thermal conductivity for H_3	0.5–4.0	0.9–4.0	0.9–1.5	1.0
Cd_1	heat capacity of minerals for H_1, 10^6 J m^{-3} K^{-1}	0.75–1.25	. . .	0.75–1.25	*0.98*
Cd_2	heat capacity of minerals for H_2, 10^6 J m^{-3} K^{-1}	0.75–1.25	. . .	0.75–1.25	*1.02*
Cd_3	heat capacity of minerals for H_3, 10^6 J m^{-3} K^{-1}	0.90–1.50	. . .	0.90–1.50	*1.21*
	Stomatal Conductance				
Rsm	minimal stomatal resistance, s m^{-1}	25–160	25–80	60–80	70
RsM	maximal stomatal resistance, s m^{-1}	3500–7000	. . .	3500–7000	5000
Rp	total plant resistance, 10^{12} s m^{-1}	0.5–5.0	0.5–2.0	1.5–2.0	1.0
PFC	critical leaf water potential, m	−170 to −110	−170 to −140	−150 to −140	−140
PST	VDP stress function parameter, 10^{-4} Pa^{-1}	1.0–5.0	1.0–2.0	1.0–2.0	2.5
	Optical Properties				
Decv	shifting of green leaves spectrum	−0.05–0.05	−0.02–0.05	−0.02–0.0	0.0
Decj	shifting of yellow leaves spectrum	−0.05–0.05	. . .	−0.05–0.05	0.0
Emif	leaf emissivity	0.96–0.99	0.98–0.99	0.98–0.99	0.985
Ass	shifting for dry soil albedo spectrum	−0.04–0.04	. . .	0.0–0.04	0.0
Ash	shifting of wet dry soil albedo spectrum	−0.04–0.04	. . .	−0.04–0.04	0.0
Wd	max 0–5 cm water content for dry soil albedo, $m^3\ m^{-3}$	0.15–0.24	0.17–0.24	0.17–0.24	0.20
Ww	min 0–5 cm water content for wet soil albedo, $m^3\ m^{-3}$	0.25–0.33	. . .	0.28–0.33	0.29
Emis	soil emissivity	0.94–0.98	0.96–0.98	0.96–0.98	0.96
Gv	visible-infrared parameter of the shielding factor	0.40–0.60	. . .	0.40–0.60	0.50
Gth	thermal infrared parameter of the shielding factor	0.70–0.90	0.70–0.85	0.75–0.85	0.85
	Root Profile				
Afdr	amplitude coef. of maximum root length density, m m^{-3}	5666–8500	. . .	5666–7800	7000
Lfdr	spreading coef. of maximum root length density	1×10^{-4}–2×10^{-4}	1×10^{-4}–1.8×10^{-4}	1×10^{-4}–1.8×10^{-4}	1.25×10^{-5}

[a]"Initial," "Intermediate," and "Final" columns indicate the initial a priori uncertainty ranges, the preferential uncertainty ranges deduced from the multiobjective generalized sensitivity analysis (MOGSA) algorithm, and the final uncertainty ranges after the multiobjective calibration iterative procedure (MCIP), respectively. Observed or calibrated (in italics) values during the Alpilles-ReSeDA experiment are indicated in the last column.

over the whole crop cycle, respectively. Unfortunately, failures in the Bowen ratio instrumentation, generating error in the system for measuring vapor and temperature gradients, did not allow the estimation of turbulent fluxes as accurately as expected. So, in this study, we only used latent and sensible heat fluxes acquired by Eddy Correlation (EC) instrumentation.

3.3. Modeling Strategy

[18] For all the SiSPAT-RS simulations, a soil column of 200 cm was layered in three horizons, corresponding to the 0–10 cm soil depth (denoted H1 hereafter), 10–30 cm (H2) and 30–200 cm (H3) soil layers. This soil description appeared relatively realistic as a first approximation for crops, according to agricultural practices (Chanzy, INRA Avignon, personal communication). The retention and hydraulic conductivity curves were parameterized using the *Van Genuchten* [1980] model and the *Brooks and Corey* [1964] model, respectively. The vegetation was modeled with two layers: a green vegetation layer and a yellow senescent vegetation layer.

[19] The multiobjective approach was performed on 35 parameters of the SiSPAT-RS model (23 for soil and 12 for vegetation). The description of these parameters is listed in Table 1. They described the thermal and hydraulic properties of the soil, the canopy stomatal regulation, the

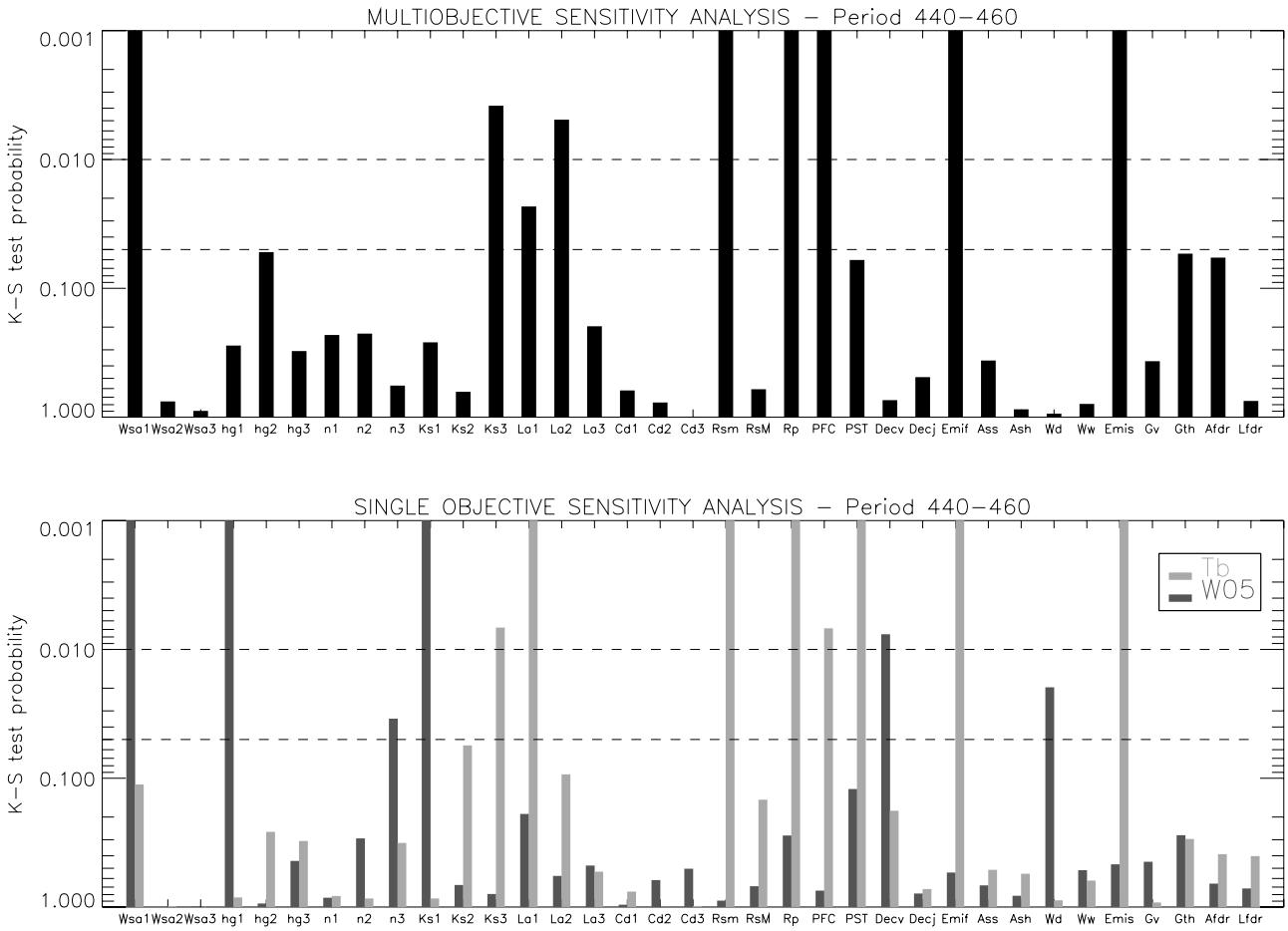

Figure 5. Multiobjective SiSPAT–Remote Sensing (RS) model sensitivity on period DOE 440–460 to the 35 input parameters. Vertical bars indicate relative sensitivity of parameters in terms of probability result of the KS test. Horizontal dashed lines indicate transition levels between "high" (above 0.01), "medium" (between 0.01 and 0.05), and "low" (under 0.05) sensitivities.

soil and vegetation optical properties and the root length density. Time-dependent input variables were not considered in this study, such as the canopy height, the green and yellow OAI. They were prescribed from ground observation, such as initial conditions. Moreover, a typical root profile was considered. An a priori uncertainty range was attributed to each of the 35 free parameters. They accounted for experimental errors and for the spatial variability observed during the Alpilles ReSeDA experiment. A uniform distribution was associated to each parameter, except for the saturated hydraulic conductivity, for which a uniform distribution was associated to the logarithm of the uncertainty range.

[20] Samples of 2500 simulations were realized. Tests were performed to verify that the size of the samples was large enough to obtain robust results [*Demarty*, 2001]. Similarly to *Leplastrier et al.* [2002], a threshold procedure on each single objective function was considered after the Pareto ranking. Threshold values for the upper 5 cm of soil and for the thermal infrared brightness temperature were simply chosen in order to assure a reasonable compromise between the numbers of "acceptable" and "non acceptable" solutions. Moreover, to well emphasize the synergy between the two assimilated variables, single-objective analyses were also performed on the SiSPAT-RS model. For consistency, the single-objective thresholds were chosen to partition the 2500 simulations into similar fraction to those achieved by the joint multiobjective sensitivity analysis [*Bastidas et al.*, 1999].

4. Results

4.1. Sensitivity Analysis

[21] Figures 5 and 6 present model sensitivity results obtained on each of the two periods with MOGSA. Each figure is composed of two subplots showing the joint multiobjective analysis (top) and the two single-objective analyses (bottom). A vertical bar indicates the model sensitivity in terms of probability result of the KS test for each of the 35 parameters. The horizontal dashed lines indicate the transition levels between "high," "medium," and "low" model sensitivity [*Bastidas et al.*, 1999]. If the vertical bar crosses the level 0.01, the model is highly sensitive to the considered parameter. Conversely, under the level 0.05, the model is insensitive to the parameter. Medium model sensitivity is considered between the levels 0.01 and 0.05.

[22] On the period DOE 440–460, multiobjective sensitivity analysis results (top part of the Figure 5) show that nine parameters had at least a medium impact on simula-

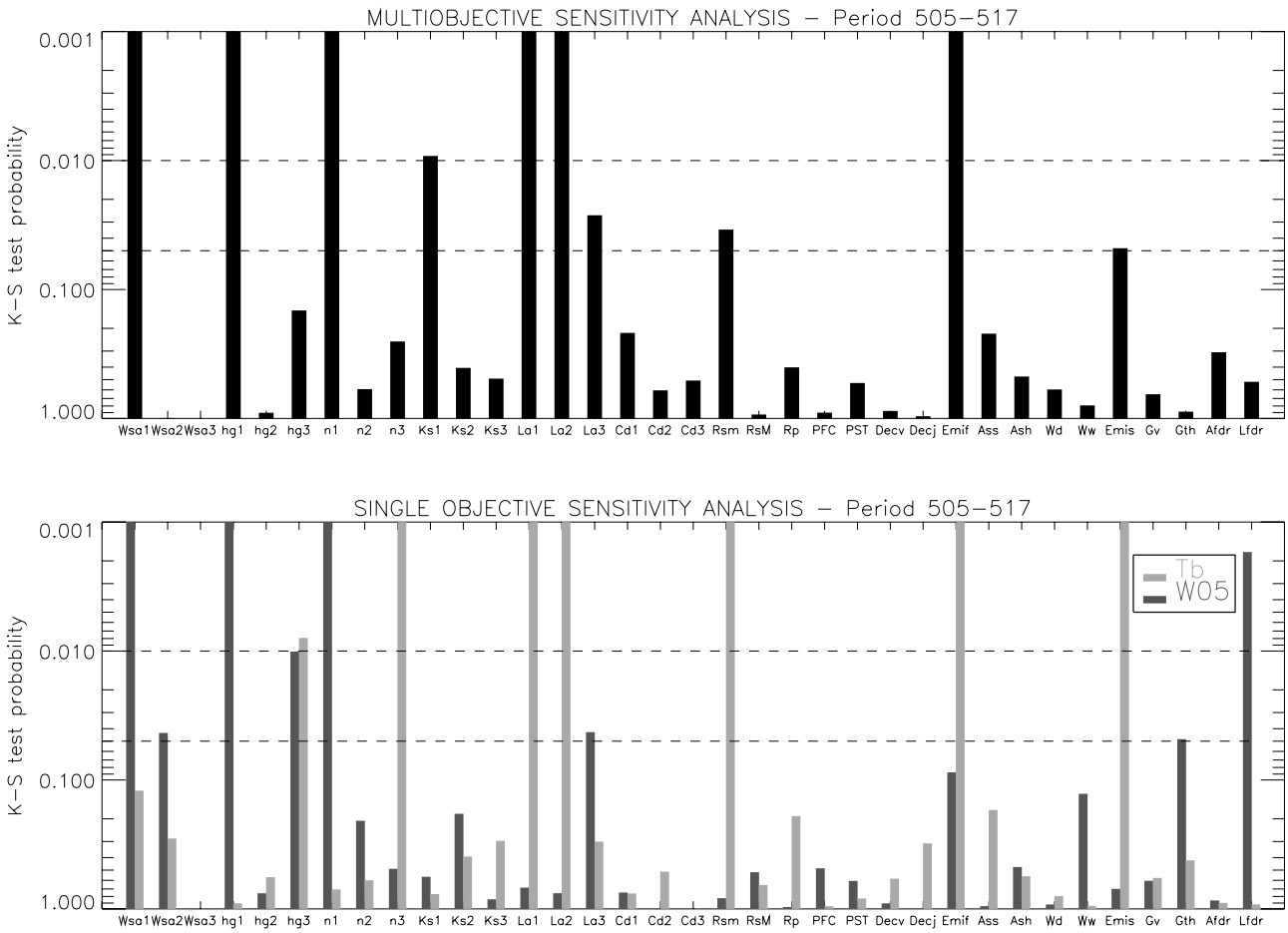

Figure 6. Same as Figure 5, but for period DOE 505–517.

tions: five parameters were related to the soil (Wsa_1, Ks_3, La_1, La_2, Emis) and four to the vegetation (Rsm, Rp, PFC, Emif). As might be expected from the knowledge of the crop development and the drying of the soil, a significant impact of the parameters controlling the stomatal regulation were found (Rsm, Rp, PFC). The Rsm parameter represented the minimal stomatal resistance when no stress occurred. The plant resistance Rp and the critical leaf water potential PFC controlled the water extraction in the soil. These three parameters were generally considered as key parameters for calibrating the SiSPAT model [*Braud et al.*, 1995; *Olioso et al.*, 2002b]. They played an important role on the simulated thermal infrared brightness temperature (bottom part of Figure 5). Similar analysis was established for the parameters controlling the thermal conductivity in soil layers between 0 and 30 cm (La_1, La_2), and for the emissivities of the soil and the vegetation (Emis, Emif). Conversely, it is important to note that the model was not really sensitive to soil hydraulic properties, since only two parameters (Ks_3, Wsa_1) were identified on the joint multiobjective sensitivity analysis. Owing to its large impact on the water exchanges in the deep soil layers, the saturated hydraulic conductivity of H3 (Ks_3) played an important role on simulations. The saturated water content of the surface horizon (Wsa_1) was the only retention curve parameter having a significant impact on the joint multiobjective sensitivity analysis. However, single-objective sensitivity analysis on the surface water content revealed that the model was also highly sensitive to the soil hydraulic properties of the surface horizon (Wsa_1, hg_1, Ks_1). More generally, we found that the joint multiobjective sensitivity analysis was close to the single-objective sensitivity analysis performed on the thermal infrared brightness temperature. This could be explained by a large internal weight giving to the threshold of the brightness temperature; this last being more discriminating for the acceptable solutions.

[23] On the period DOE 505–517, multiobjective sensitivity analysis results (Figure 6) show that 10 parameters had at least a medium impact on simulations: eight parameters were related to the soil (Wsa_1, hg_1, n_1, Ks_1, La_1, La_2, La_3, Emis) and only two to the vegetation (Rsm, Emif). These results were consistent with the studied environmental conditions. High model sensitivity was observed for all the soil parameters describing horizon 1 (Wsa_1, hg_1, n_1, Ks_1). As expected for a very dry soil, the parameter n had a significant impact. Similar results were found by *Demarty et al.* [2004a, 2004b]. For stomatal regulation, only the minimum stomatal resistance Rsm had a high impact on the simulation of the brightness temperature. Moreover, the parameters controlling the thermal conductivity in H1 and H2 (La_1, La_2) and soil and vegetation emissivities (Emis, Emif) had a large impact on T_b. For this period, a good agreement between the multiobjective and the two single-objective sensitivity analysis was observed.

[24] In spite of the quite similar environmental conditions in the two temporal windows, the results obtained above

revealed model sensitivity to different parameters. Thus the first period was useful to identify the main vegetation parameters during the growing period, while the second period allowed a more efficient identification of the soil properties in relation with the soil moisture level. However, some parameters (Wsa1, La1, La2, Rsm) had a significant impact on both periods. A high model response was also observed for the parameters controlling simultaneously surface soil moisture and thermal infrared brightness temperature. In particular, it was established that the parameters describing the stomatal regulation and the soil water exchanges near the surface as well as in deeper soil layers were sensitive. More generally, the six above sensitivity analyses (1 multiobjective and two single-objective for each of the two temporal windows) allowed the identification of 21 main influential parameters. These results underlined the potential of T_b and W_{05} to retrieve information on many input parameters used in a physically SVAT model. Next section focuses on the way to assimilate these variables in the model.

4.2. Assimilation of the W_{05} and T_b Variables

[25] Using the six previous sensitivity analyses, we determined the preferential uncertainty ranges of the 21 main influential parameters (Table 1, ''Intermediate'' column). In general, a more efficient narrowing of the a priori uncertainty range was associated to high model sensitivity. A typical example was the minimal stomatal resistance (Rsm), which had a large influence in multiobjective and single-objective analyses on T_b for the two temporal windows. Rsm originally ranged between 25–160 s m^{-1}; it was constrained to its lowest values, between 25 and 80 s m^{-1}, according to the multiobjective sensitivity analysis on period 440–460 which provided the more efficient contraction of the initial feasible space. Other main example concerned the scale factor of the VG retention model of H1 (h_1) that was constrained to intermediate values of its initial range. In fact, these values appeared the most appropriate to improve the surface soil moisture critter, since the single-objective sensitivity analyses on W_{05} that was carried out on period 440–460 and period 505–517, narrowed initial range to the lowest values and the highest values, respectively. Nevertheless, this case was atypical, since no contradiction in uncertainty ranges was observed between the various sensitivity studies for all the others parameters.

[26] This analysis of preferential uncertainty ranges provided quantitative information for calibrating the SVAT model. However, the preferential ranges of the 21 parameters were still relatively large. Moreover, no sensitivity was observed for 14 of the 35 parameters. In order to progress toward the optimization of the 35 input parameters, the multiobjective calibration iterative procedure (MCIP, see section 2.3) was applied on the SiSPAT-RS model. As MOGSA results showed that the two separate periods provided quite close results in terms of model sensitivity, we decided to test MCIP on the period DOE 440–460 only, using the preferential uncertainty ranges observed for the 21 ''influential'' parameters. The 14 parameters for which no sensitivity was observed were let free to vary in their a priori ranges. Two new iterations (see Figure 3) were performed with MCIP. Results are described as follows.

[27] Figure 7 shows the MCIP performance in terms of the RMSE of W_{05} and T_b. Each subfigure represents a specific iteration. The partition into ''acceptable'' and ''non acceptable'' solutions and the threshold values are indicated. Results showed that the performance of the MCIP increased with the successive iterations. At the third iteration, the whole set of the 2500 simulations provided relatively similar RMSE, revealing that the number of iterations was sufficient. For each iteration, RMSE around 0.9 K were systematically obtained on T_b. Conversely, many sets of parameters allowed the assessment of very low RMSE on W_{05}.

[28] Figure 8 presents the impact of the assimilation procedure on the simulated sensible (H) and latent (LE) heat fluxes. Both H and LE were improved with the successive iteration. The scattering of the RMSE regularly decreased from 50–70 Wm^{-2} to 10–20 Wm^{-2}. The RMSE on H and LE were finally around 25–40 Wm^{-2}. They were relatively close to the measurement errors around of 30 Wm^{-2} which were estimated on the turbulent fluxes during the Alpilles-ReSeDA experiment [*Olioso et al.*, 2002a]. It was observed that the improvement of the simulation of the turbulent fluxes was mainly due to the use of the brightness temperature (not shown in this study). Such a high correlation between the surface fluxes and the brightness temperature was in good agreement with the environmental conditions at the time of the analysis, which were characterized by a growing vegetation during an event of soil drying, for which water stress occurred. In the cases of uncompleted canopy or senescence, the account of W_{05} in the multiobjective procedure could have a higher impact in the simulation of the surface turbulent fluxes, and might be also a good mean to assess and control the partition of evapotranspiration into evaporation and transpiration. Furthermore, the sensitivity analyses were shown that the W_{05} variable allowed the retrieval of the hydraulic properties. These properties had a high impact on the control of infiltration toward deeper soil layers, and as a consequence on the available water content for transpiration. So, especially during or after a rain event, the account of W_{05} could have a higher influence on the assessment of the turbulent fluxes.

[29] The final ranges of the SiSPAT-RS parameters are shown in Table 1 (''Final'' column). On one hand, it was not possible to reduce the initial a priori uncertainty ranges of only eight parameters, such as the soil heat capacity of the three horizons (Cd_1, Cd_2, Cd_3) or the maximal stomatal resistance (RsM). These parameters had a very low impact on the simulations of the two variables used for the calibration process (T_b and W_{05}). On the other hand, 27 parameters were highly optimized, revealing two main key findings. First, it was possible to improve the optimization of the 21 influential parameters that were obtained using MOGSA in section 4.1. For some of the parameters, narrow final ranges were particularly found, as for example for the minimal stomatal resistance Rsm (60–80 s m^{-1}) and for the critical leaf water potential PFC (−150 to −140 m). Second, six additional parameters were optimized, such as the parameters describing the retention curve of H2 (hg_2, n_2). This showed that the model sensitivity was affected by the successive contractions of the feasible parameter space. Figure 9 shows an example of model sensitivity obtained

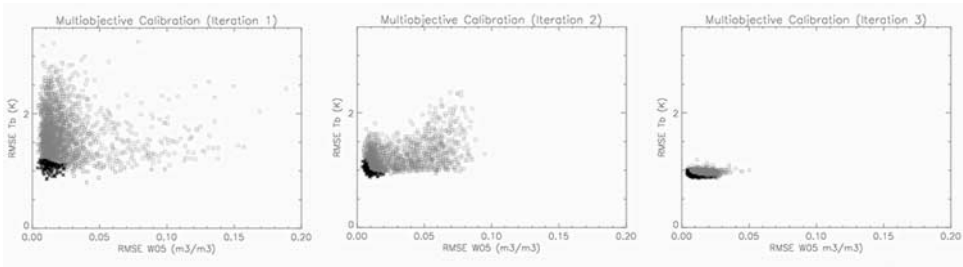

Figure 7. Performance of the MCIP in terms of RMSE of the surface water content (W_{05}) and the local brightness temperature (T_b). Each subfigure shows "acceptable" (black asterisk) and "nonacceptable" (gray square) simulations for a specific iteration. Thresholds of 1.2 K and 0.025 m^3 m^{-3} were considered for T_b and W_{05}.

for iteration 2. It can be compared to Figure 5 in order to emphasize relative changes in model sensitivity. Moreover, the comparison between the optimized parameters and the values derived from Alpilles-ReSeDA experiment by *Olioso et al.* [2002a, 2002b] ("Observed" column in Table 1) showed a very good agreement. The main differences concerned the soil hydraulic properties of H2 (hg_2, n_2, Ksa_2) for which large final ranges were found. These results, revealing the potential of the two T_b and W_{05} for constraining a physically based SVAT model, opened perspectives on the combined assimilation of the passive microwave and thermal infrared observations.

[30] Figure 10 shows the impact of the parameter calibration on the simulated energy fluxes and soil water content. For the turbulent fluxes, as expected from Figure 8, a good agreement was found between simulated and observed values. More differences were observed on the water content of the soil layers between 30 and 50 cm. This was partially explained by the large ranges of hydraulic soil properties of H2 (10–30 cm). Conversely, water content of the deep layers was well simulated, in agreement with the high model sensitivity to the parameters controlling water exchanges in deep soil layers and stomatal regulation.

5. Conclusions and Discussion

[31] This study presents a multiobjective approach to retrieve surface information of a physically based SVAT model through the knowledge of surface water content (W_{05}) and thermal infrared brightness temperature (T_b) measurements as calibration variables. The approach used a new multiobjective procedure, called the multiobjective calibration iterative procedure (MCIP). This procedure is based on the ability of the multiobjective generalized sensitivity analysis (MOGSA [*Bastidas et al.*, 1999]) to identify and quantify the main influential parameters on the simulations of W_{05} and T_b. The Simple Soil Plant Atmosphere Transfer–Remote Sensing (SiSPAT-RS [*Braud et al.*, 1995; *Demarty et al.*, 2004b]) model and the database acquired on a winter wheat field during the Alpilles ReSeDA experiment [*Olioso et al.*, 2002a] are used in this study.

[32] The analysis of model sensitivity being a key issue both for investigating the model structure and for isolating the main influential parameters, a sensitivity analysis of the SiSPAT-RS model to 35 input parameters was first carried out with MOGSA on two separate temporal windows among the wheat crop cycle (see Figures 5 and 6). Although these two temporal windows are not really contrasted in terms of environmental conditions, results showed slightly differing behavior in model sensitivity. The model was very sensitive to the parameters controlling both W_{05} and T_b. More specifically; it was shown that W_{05} and T_b were useful to identify the hydraulic and thermal properties of the surface soil horizon and the main vegetation parameters, respectively. Such an association of these two variables was very interesting for constraining the main surface processes, such as stomatal regulation and soil water exchanges near the surface as well as in deeper soil layers. Furthermore, the MOGSA algorithm was also useful to provide quantitative information on these main parameters in terms of preferential ranges. As by *Demarty et al.* [2004a, 2004b], it was particularly that these a posteriori preferential ranges could be still relatively large, implying difficulties for choosing calibrated values.

[33] In order to progress toward the optimization of model parameters, a new multiobjective procedure MCIP was applied in a second step to SiSPAT-RS. Results showed that MCIP is an original and pertinent approach for improving calibration (i.e., reducing the a posteriori prefer-

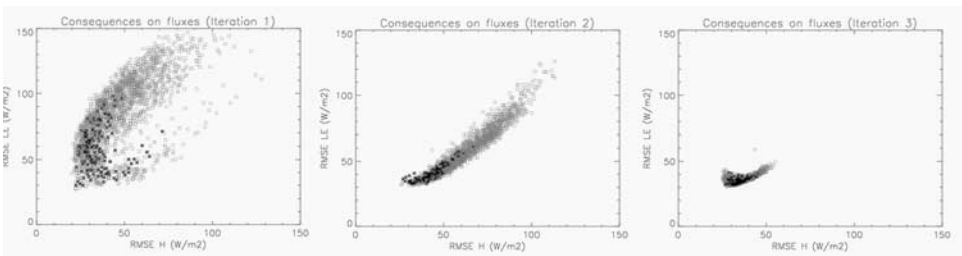

Figure 8. Impact of the MCIP on the simulated sensible (H) and latent (LE) heat fluxes.

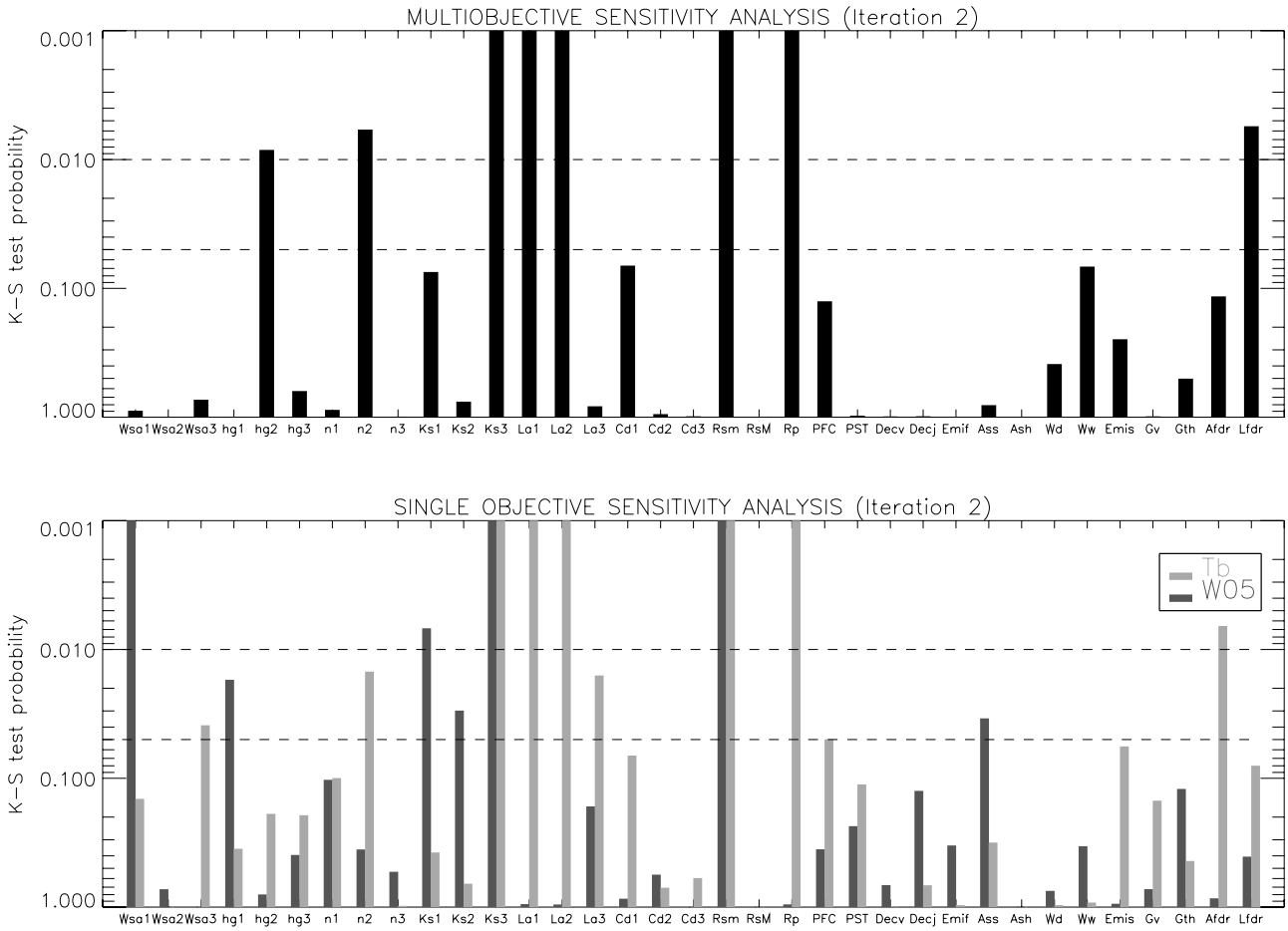

Figure 9. Multiobjective SiSPAT-RS model sensitivity for iteration 2 and on period DOE 440–460 to the 35 parameters. Comparison with Figure 5 shows relative changes in model sensitivity after contraction of the feasible parameter space. See legend of Figure 5.

ential ranges) in the case of this complex model. The new multiobjective approach seems well suited for complex models, which require the prescription of many input parameters, are time consuming and for which another multiobjective approach can not be reasonable in terms of amount of simulations required by the optimization procedure. Thus in regard with the 100 000 simulations generally required by a multiobjective calibration with the MOCOM-UA algorithm [*Yapo et al.*, 1998; *Gupta et al.*, 1999], MCIP only required the generation of 7500 simulations in our studied case. Such a number of simulations is compatible with a good computational efficiency of the SiSPAT-RS model. Moreover, it was particularly shown that the parameter retrieval with MCIP was in good agreement with the observed values during the Alpilles-ReSeDA experiment and had a positive impact on the simulation of the main surface processes, such as the sensible (H) and latent (LE) heat fluxes and the soil water content.

[34] In this study, we expected that W_{05} and T_b would be two useful and complementary variables for retrieving quantitative information on surface properties. In terms of parameter retrieval, results clearly showed that these two variables were complementary. More specifically, it was shown that the model sensitivity was affected by the successive contractions of the feasible parameter space. However, in terms of impact on the turbulent heat fluxes, it was observed that the thermal infrared brightness temperature was the main variable providing significant information (see Figure 8). This was a direct consequence of the environmental conditions, characterized by growing vegetation during an event of soil drying, for which water stress occurred (see Figure 10). Indeed, in these conditions, brightness temperature is highly correlated to evapotranspiration flux. Concerning water transfers in the soil, it was shown that both W_{05} and T_b provided information on the soil hydrodynamic properties which drive these transfers. This was true at the first iteration (see above the discussion on the sensitivity analysis with MOGSA, Figures 5 and 6), but also at the following iterations (as presented for iteration 2 in Figure 9). If these properties were not retrieved accurately, it would be not possible to obtain right simulation of latent heat flux on the long term [*Olioso et al.*, 2002b; *Demarty et al.*, 2004b]. It may also be possible that in other environmental situations, such as for less developed canopies, senescence or rain events (not studied here), the impact of W_{05} on the calibration of the model for the simulation of turbulent heat fluxes was higher than in the present study. This is to be investigated in the future. New studies have already been initiated applying MCIP to the ISBA-Ags model [*Calvet et al.*, 1998], showing that the combined use of 1.4 GHz and thermal infrared brightness temperatures made it possible to retrieve most of the

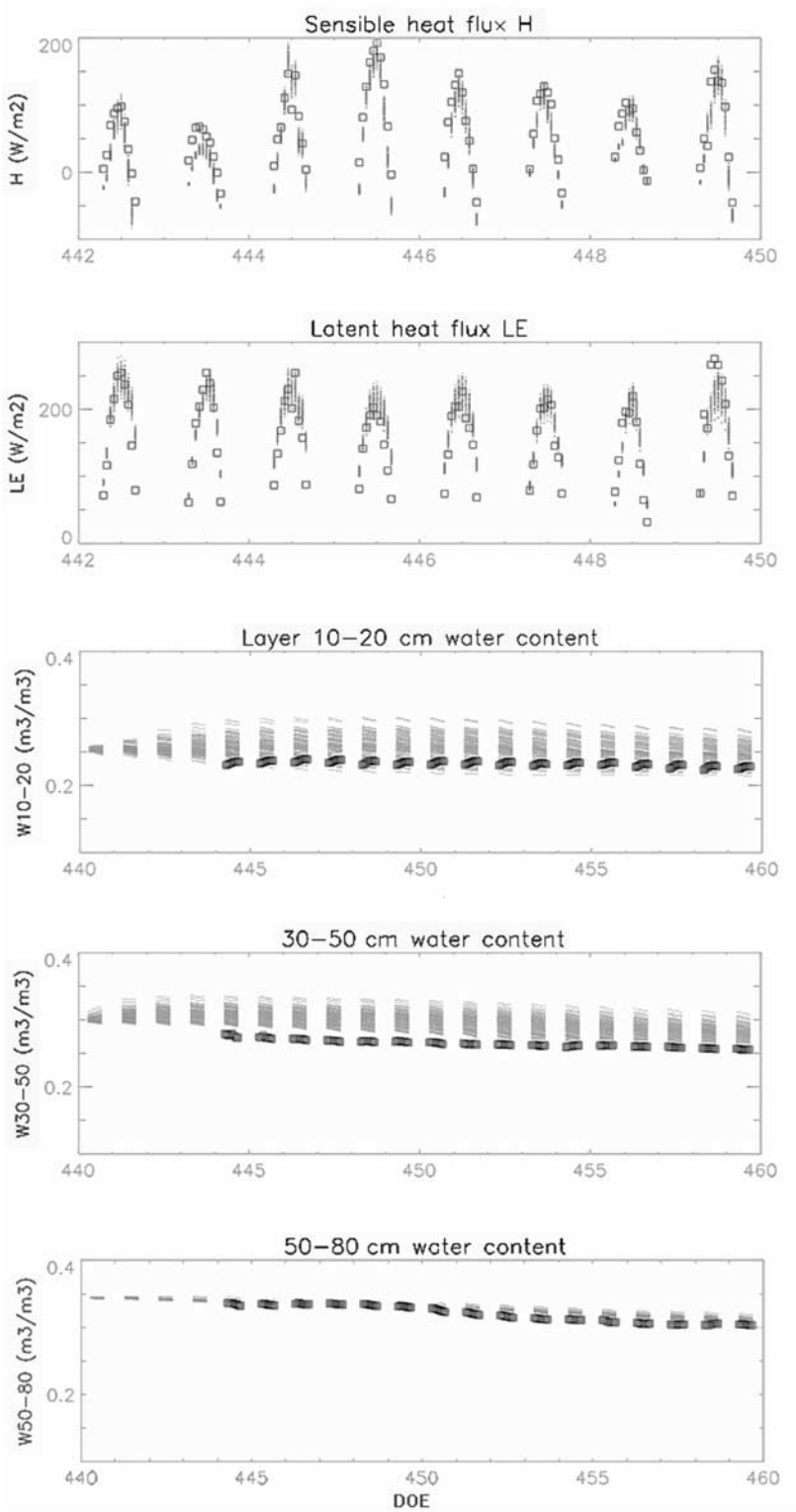

Figure 10. Performance of the final "acceptable" solutions (gray), according to the available Alpilles ReSeDA observations (black square), on the turbulent surface fluxes (for only 8 days) and on various soil water contents (for the whole studied period of 20 days).

model input parameters [*Demarty et al.*, 2004a], Using only one of these remote sensed variables resulted in wrong determination of the parameters and erroneous simulation of evapotranspiration.

[35] MCIP was used here in a context of remotely sensed data. This study opens perspectives for the combined use of various multispectral remotely sensed observations, such as passive microwaves and thermal infrared signals, in a SVAT

model. We did not account for the issue of the spatiotemporal resolution of satellite sensors. The main advantage of data assimilation is its ability to merge spatially distributed information obtained from many sources with different resolutions, coverage and uncertainties [*Margulis et al.*, 2002]. Further investigations need to be performed toward this objective. In particular, on the temporal aspect, an analysis must be performed, as by *Calvet and Noilhan* [2000] for example, in order to determine the required frequency of the assimilated observations and its impact on the driving of the SVAT model. The issue of the spatial resolution of the satellite sensors might be approached using disaggregated remotely sensed data (or products, such as soil moisture) at the scale of the various entities constituting the mixed pixel [*Pellenq et al.*, 2003; *Kustas et al.*, 2003]. Another way might be the direct assimilation of the satellite observations at the level of the mixed pixel. In this case, the multiobjective procedure must be able to constrain the model on each of the entities constituting the mixed pixel. Few recent studies have been focused on the potential of approaches allowing the retrieval of many input parameters, as in the case of the distributed land surface properties of heterogeneous pixels [*Burke et al.*, 2002; *Crow and Wood*, 2003]. Nevertheless, the Monte Carlo nature of the multiobjective approaches requiring multiple simulations could make them less practical than another technique. This emphasizes the development of alternative approach, such as MCIP, that allows the assessment of many input parameters through a relative low number of simulations.

[36] The last main assumption considered in this study concerned the time-dependent input variables (LAI and canopy height) which were prescribed from in situ observations. Although *Demarty et al.* [2004b] showed that these variables had an impact on model sensitivity; this was not trivial to simply take them into account in the multiobjective approach. Moreover, SVAT model were not initially designed to simulate such variables. This emphasizes the usefulness to couple a vegetation growth model with a SVAT model [*Cayrol et al.*, 2000; *Olioso et al.*, 2005]. Thus further works must concern the assimilation of satellite observations in a coupled SVAT–vegetation growth model, according to their time and spatial resolutions.

[37] **Acknowledgments.** The authors would like especially to thank all the partners of the Alpilles-ReSeDA program for providing ground truth data. The Alpilles-ReSeDA project was funded by the ECC-EG XII (contract ENV4-CT96-0326-PL952071) and the INSU/CNRS French national programs (PNRH and PNTS). Jérôme Demarty would like to dedicate this paper to Paul.

References

Bastidas, L. A., H. V. Gupta, S. Sorooshian, W. J. Shuttleworth, and Z. L. Yang (1999), Sensitivity analysis of a land surface scheme using multicriteria methods, *J. Geophys. Res.*, *104*, 19,481–19,490.

Boyle, D. P., H. V. Gupta, and S. Sorooshian (2000), Toward improved calibration of hydrologic models: Combining the strengths of manual and automatic methods, *Water Resour. Res.*, *36*, 3663–3674.

Boyle, D. P., H. V. Gupta, S. Sorooshian, V. Koren, Z. Zhang, and M. Smith (2001), Toward improved streamflow forecasts: Value of semidistributed modeling, *Water Resour. Res.*, *37*, 2749–2759.

Braud, I. (2000), *SiSPAT: A Numerical Model of Water and Energy Fluxes in the Soil-Plant-Atmosphere Continuum, Version 3.0, SiSPAT User's Manual*, 107 pp., Lab. d'Étude des Transferts en Hydrol. et Environ., Grenoble, France.

Braud, I., A. C. Dantas-Antonino, M. Vauclin, J. L. Thony, and P. Ruelle (1995), A simple soil-plant-atmosphere transfer model (SiSPAT) development and field verification, *J. Hydrol.*, *166*, 213–250.

Brooks, R. H., and A. T. Corey (1964), Hydraulic properties of porous media, report, Colo. State Univ., Fort Collins.

Burke, E. J., R. J. Gurney, L. P. Simmonds, and T. J. Jackson (1997), Calibrating a soil water and energy budget model with remotely sensed data to obtain quantitative information about the soil, *Water Resour. Res.*, *33*, 1689–1697.

Burke, E. J., R. J. Gurney, L. P. Simmonds, and P. E. O'Neill (1998), Using a modeling approach to predict soil hydraulic properties from passive microwave measurements, *IEEE Trans. Geosci. Remote Sens.*, *36*, 454–462.

Burke, E. J., L. A. Bastidas, and W. J. Shuttleworth (2002), Exploring the potential for multipatch soil moisture retrievals using multiparameter optimization techniques, *IEEE Trans. Geosci. Remote Sens.*, *40*, 1114–1120.

Calvet, J. C., and J. Noilhan (2000), From near-surface to root-zone soil moisture using year-round data, *J. Hydrometeorol.*, *1*, 393–411.

Calvet, J. C., J. Noilhan, J. L. Roujean, P. Bessemoulin, M. Cabelguenne, A. Olioso, and J. P. Wigneron (1998), An interactive vegetation SVAT model tested against data from six contrasting sites, *Agric. For. Meteorol.*, *92*, 73–95.

Camillo, P. (1991), Using one- and two-layer models for evaporation estimation with remotely sensed data, in *Land Surface Evaporation: Measurement and Parameterization*, pp. 183–197, Springer, New York.

Carlson, T., E. Perry, and T. Schmugge (1990), Remote estimation of soil moisture availability and fractional vegetation cover for agricultural fields, *Agric. For. Meteorol.*, *52*, 45–69.

Cayrol, P., L. Kergoat, S. Moulin, G. Dedieu, and A. Chehbouni (2000), Calibrating a coupled SVAT-vegetation growth model with remotely sensed reflectance and surface temperature—A case study for the HAPEX-Sahel grassland sites, *J. Appl. Meteorol.*, *39*, 2452–2472.

Clevers, J. G. P. W., and H. J. C. van Leeuwen (1996), Combined use of optical and microwave remote sensing data for crop growth monitoring, *Remote Sens. Environ.*, *56*, 42–51.

Crow, W., and E. F. Wood (2003), The assimilation of remotely sensed soil brightness temperature imagery into a land surface model using Ensemble Kalman filtering: A case study based on ESTAR measurements during SGP97, *Adv. Water Resour.*, *26*, 137–149.

Demarty, J. (2001), Développement et application du modèle SiSPAT-RS à l'échelle de la parcelle dans le cadre de l'expérience Alpilles ReSeDA, M.S. thesis, 220 pp., Univ. Paris 7, France.

Demarty, J., C. Ottlé, C. François, I. Braud, and J. P. Frangi (2002), Effect of aerodynamic resistance modeling on SiSPAT-RS simulated surface fluxes, *Agronomie*, *22*, 641–650.

Demarty, J., A. Olioso, O. Marloie, and V. Rivalland (2004a), Etalonnage et validation de modèles de surface au moyen d eméthodes stochastiques et muticritère, part 1: Développement et évaluation à l'échelle locale, paper presented at Atelier de Modélisation de l'Atmosphère, Toulouse, France, 28–29 Nov.

Demarty, J., C. Ottlé, I. Braud, A. Olioso, J. P. Frangi, L. Bastidas, and H. V. Gupta (2004b), Using a multiobjective approach to retrieve information on surface properties used in a SVAT model, *J. Hydrol.*, *287*, 214–236.

Droogers, P., and W. Bastiaanssen (2002), Irrigation performance using hydrological and remote sensing modeling, *J. Irrig. Drainage Eng.*, *128*, 11–18.

Federer, C. A. (1979), A soil-plant-atmosphere model for transpiration and availability of soil water, *Water Resour. Res.*, *15*, 555–562.

François, C., C. Ottlé, and L. Prévot (1997), Analytical parameterization of canopy directional emissivity and canopy directional radiance in the thermal infrared: Application on the retrieval of soil and foliage temperatures using two directional measurements. part 1. Theory, *Int. J. Remote Sens.*, *18*, 2587–2621.

Goldberg, D. E. (1989), *Genetic Algorithms in Search Optimization and Machine Learning*, Addison-Wesley, Boston, Mass.

Gupta, H. V., S. Sorooshian, and P. O. Yapo (1998), Toward improved calibration of hydrologic models: Multiple and noncommensurable measures of information, *Water Resour. Res.*, *34*, 751–763.

Gupta, H. V., L. A. Bastidas, S. Sorooshian, W. J. Shuttleworth, and Z. L. Yang (1999), Parameter estimation of a land surface scheme using multicriteria methods, *J. Geophys. Res.*, *104*, 19,491–19,503.

Gupta, H. V., L. Bastidas, J. A. Vrugt, and S. Sorooshian (2003), Multiple criteria global optimization for watershed model calibration, in *Calibration of Watershed Models*, *Water Sci. Appl. Ser.*, vol. 6, edited by Q. Duan et al., pp. 125–132, AGU, Washington, D. C.

Houser, P. R., H. V. Gupta, W. J. Shuttleworth, and J. S. Famiglietti (2001), Multiobjective calibration and sensitivity of a distributed land surface water and energy balance model, *J. Geophys. Res.*, *106*, 33,421–33,433.

Jackson, T. J., and T. J. Schmugge (1991), Vegetation effects on the microwave emission of soils, *Remote Sens. Environ.*, *36*, 203–212.

Jackson, T. J., D. M. LeVine, C. T. Swift, T. J. Schmugge, and F. R. Scheibe (1995), Large area mapping of soil moisture using the ESTAR passive microwave radiometer in Washita '92, *Remote Sens. Environ.*, *53*, 27–37.

Jackson, T. J., D. M. LeVine, A. Y. Hsu, A. Oldak, P. J. Starks, C. T. Swift, J. D. Isham, and M. Haken (1999), Soil moisture mapping at regional scales using microwave radiometry: The Southern Great Plains Hydrology Experiment, *IEEE Trans. Geosci. Remote Sens.*, *37*, 2136–2151.

Jarvis, P. G. (1976), The interpretation of the variations in leaf water potential and stomatal conductance found in canopies in the field, *Philos. Trans. R. Soc. London, Ser. B*, *273*, 593–602.

Kustas, P. W., J. M. Norman, M. C. Anderson, and A. N. French (2003), Estimating subpixel surface temperatures and energy fluxes from the vegetation index-radiometric temperature relationship, *Remote Sens. Environ.*, *85*, 429–440.

Leplastrier, M., A. J. Pitman, H. Gupta, and Y. Xia (2002), Exploring the relationship between complexity and performance in a land surface model using the multicriteria method, *J. Geophys. Res.*, *107*(D20), 4443, doi:10.1029/2001JD000931.

Madsen, H. (2000), Automatic calibration of a conceptual rainfall-runoff model using multiple objectives, *J. Hydrol.*, *235*, 276–288.

Margulis, S. A., and D. Entekhabi (2003), Variational assimilation of radiometric surface temperature and reference-level micrometeorology into a model of the atmospheric boundary layer and land surface, *Mon. Weather Rev.*, *131*, 1272–1288.

Margulis, S. A., D. McLaughlin, D. Entekhabi, and S. Dunne (2002), Land data assimilation and estimation of soil moisture using measurements from the Southern Great Plains 1997 Field Experiment, *Water Resour. Res.*, *38*(12), 1299, doi:10.1029/2001WR001114.

Meixner, T., L. A. Bastidas, H. V. Gupta, and R. C. Bales (2002), Multicriteria parameter estimation for models of stream chemical composition, *Water Resour. Res.*, *38*(3), 1027, doi:10.1029/2000WR000112.

Milly, P. C. D. (1982), Moisture and heat transport in hysteretic inhomogeneous porous media: A matric head-based formulation and a numerical model, *Water Resour. Res.*, *18*, 489–498.

Olioso, A., H. Chauki, D. Courault, and J. P. Wigneron (1999a), Estimation of evapotranspiration and photosynthesis by assimilation of remote sensing data into SVAT models, *Remote Sens. Environ.*, *68*, 341–356.

Olioso, A., H. Chauki, J.-P. Wigneron, P. Bertuzzi, A. Chanzy, P. Bessemoulin, and J.-C. Calvet (1999b), Estimation of energy fluxes from thermal infrared, spectral reflectances, microwave data and SVAT modeling, *Phys. Chem. Earth, Part B*, *24*, 829–836.

Olioso, A., Y. Inoue, J. P. Wigneron, S. Ortega-Farias, P. Lecharpentier, M. Pardé, J. C. Calvet, and O. Inizan (2001), Using a coupled crop-SVAT model to assess crop canopy processes from remote sensing data, paper presented at IGARSS, Sydney, Australia.

Olioso, A., et al. (2002a), SVAT modeling over the Alpilles-ReSeDA experiment: Experimental setup for monitoring energy and mass transfers, *Agronomie*, *22*, 651–668.

Olioso, A., et al. (2002b), SVAT modeling over the Alpilles-ReSeDA experiment: Comparison of SVAT models, first results on wheat, *Agronomie*, *22*, 597–610.

Olioso, A., et al. (2005), Future directions for advanced evapotranspiration modeling: Assimilation of remote sensing data into crop simulation models and SVAT models, *Irrig. Drainage Syst.*, in press.

Ottlé, C., and D. Vidal-Madjar (1994), Assimilation of soil moisture inversed from infrared remote sensing in a hydrological model over the Hapex-Mobilhy region, *J. Hydrol.*, *158*, 241–264.

Pellenq, J., J. Kalma, G. Boulet, G.-M. Saulnier, S. Wooldridge, Y. Kerr, and A. Chehbouni (2003), A disaggregation scheme for soil moisture based on topography and soil depth, *J. Hydrol.*, *276*, 112–127.

Shuttleworth, W. J., and R. J. Gurney (1990), The theoretical relationship between foliage temperature and canopy resistance in sparse crops, *Q. R. J. Meteorol. Soc.*, *116*, 497–519.

Soer, G. J. R. (1980), Estimation of regional evapotranspiration and soil moisture conditions using remotely sensed crop surface temperature, *Remote Sens. Environ.*, *9*, 27–45.

Taconet, O., A. Olioso, M. B. Mehrez, and N. Brisson (1995), Seasonal estimation of evaporation and stomatal conductance over a soybean field using surface IR temperatures, *Agric. For. Meteorol.*, *73*, 321–337.

Van Genuchten, M. T. (1980), A closed equation for predicting the hydraulic conductivity of unsaturated soils, *Soil Sci. Soc. Am. J.*, *44*, 892–898.

Verhoef, W. (1984), Light scattering by leaf layers with application to canopy reflectance modelling: The SAIL model, *Remote Sens. Environ.*, *16*, 125–141.

Verhoef, W. (1985), Earth Observation Modeling based on layer scattering matrices, *Remote Sens. Environ.*, *17*, 165–178.

Vrugt, J. A., H. V. Gupta, L. A. Bastidas, W. Bouten, and S. Sorooshian (2003a), Effective and efficient algorithm for multiobjective optimization of hydrologic models, *Water Resour. Res.*, *39*(8), 1214, doi:10.1029/2002WR001746.

Vrugt, J. A., H. V. Gupta, W. Bouten, and S. Sorooshian (2003b), A Shuffled Complex Evolution Metropolis algorithm for optimization and uncertainty assessment of hydrologic model parameters, *Water Resour. Res.*, *39*(8), 1201, doi:10.1029/2002WR001642.

Weiss, M., D. Troufleau, F. Baret, H. Chauki, L. Prévot, A. Olioso, N. Bruguier, and N. Brisson (2001), Coupling canopy functioning and radiative transfer models for remote sensing data assimilation, *Agric. For. Meteorol.*, *108*, 113–128.

Wigneron, J. P., A. Chanzy, J. C. Calvet, and N. Bruguier (1995), A simple algorithm to retrieve soil moisture and vegetation biomass using passive microwave measurements over crop fields, *Remote Sens. Environ.*, *51*, 331–341.

Wigneron, J.-P., J.-C. Calvet, and Y. Kerr (1996), Monitoring water interception by crop fields from passive microwave observations, *Agric. For. Meteorol.*, *80*, 177–194.

Wigneron, J.-P., A. Chanzy, J.-C. Calvet, A. Olioso, and Y. Kerr (2002), Modeling approaches to assimilating *L* band passive microwave observations over land surfaces, *J. Geophys. Res.*, *107*(D14), 4219, doi:10.1029/2001JD000958.

Xia, Y., A. J. Pitman, H. V. Gupta, M. Lepastrier, A. Henderson-Sellers, and L. A. Bastidas (2002), Calibrating a land surface model of varying complexity using multi-criteria methods and the Cabauw data set, *J. Hydrometeorol.*, *3*, 181–194.

Yapo, P. O., H. V. Gupta, and S. Sorooshian (1996), Automatic calibration of conceptual rainfall-runoff models: Sensitivity to calibration data, *J. Hydrol.*, *181*, 23–48.

Yapo, P. O., H. V. Gupta, and S. Sorooshian (1998), Multi-objective global optimization for hydrologic models, *J. Hydrol.*, *204*, 83–97.

L. A. Bastidas, Department of Civil and Environmental Engineering, Utah State University, Logan, UT 84322-8200, USA. (luis.bastidas@usu.edu)

I. Braud, Unité de Recherche Hydrologie-Hydraulique, Cemagref, 3 bis, Quai Chauveau, CP 220, F-69336 Lyon Cedex 9, France. (braud@lyon.cemagref.fr)

J. Demarty, and C. Ottlé, Centre d'étude des Environnements Terrestre et Planétaires/Centre National de la Recherche Scientifique/Université de Versailles Saint-Quentin-en-Yvelines, Avenue de l'Europe, F-78140 Vélizy, France. (jdemarty@avignon.inra.fr; ottle@cetp.ipsl.fr)

J. P. Frangi, Laboratoire Environnement et Développement/Université Paris 7, 2 place Jussieu, F-75251 Paris Cedex 5, France. (frangi@ccr.jussieu.fr)

H. V. Gupta, Sustainability of Semi-arid Hydrology and Riparian Areas, Department of Hydrology and Water Resources, University of Arizona, Tucson, AZ 85721-0011, USA. (hoshin@hwr.arizona.edu)

A. Olioso, Unité CSE, Institut National de la Recherche Agronomique Avignon, F-84914 Avignon Cedex 9, France. (olioso@avignon.inra.fr)